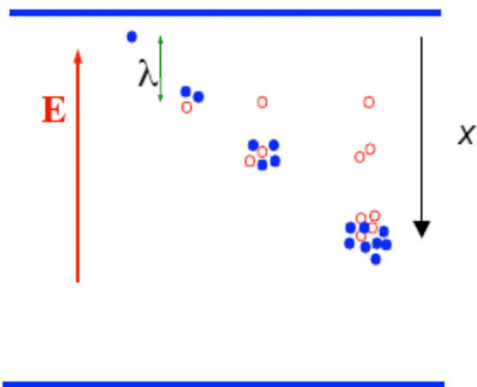


## AVALANCHE MULTIPLICATION IN UNIFORM FIELD

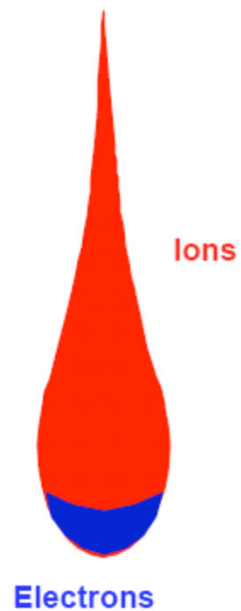


$$dn = n \alpha dx$$

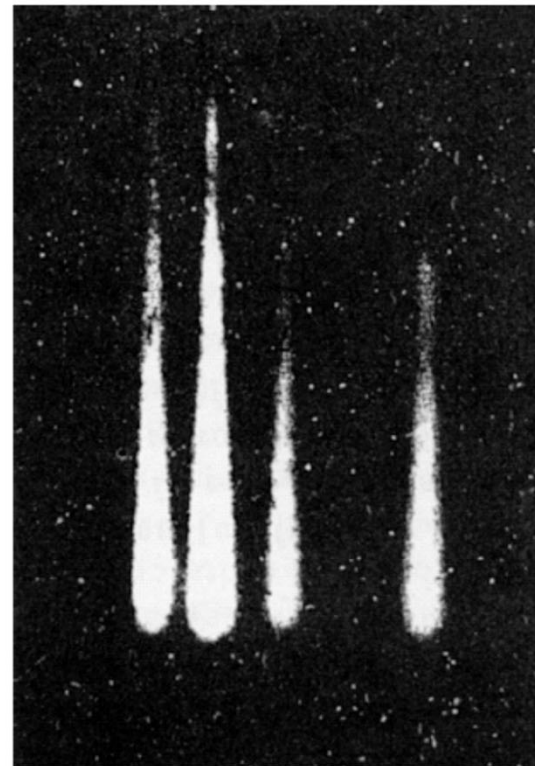
$$n(x) = n_0 e^{\alpha x}$$

Multiplication factor or Gain

$$M(x) = \frac{n}{n_0} = e^{\alpha x}$$

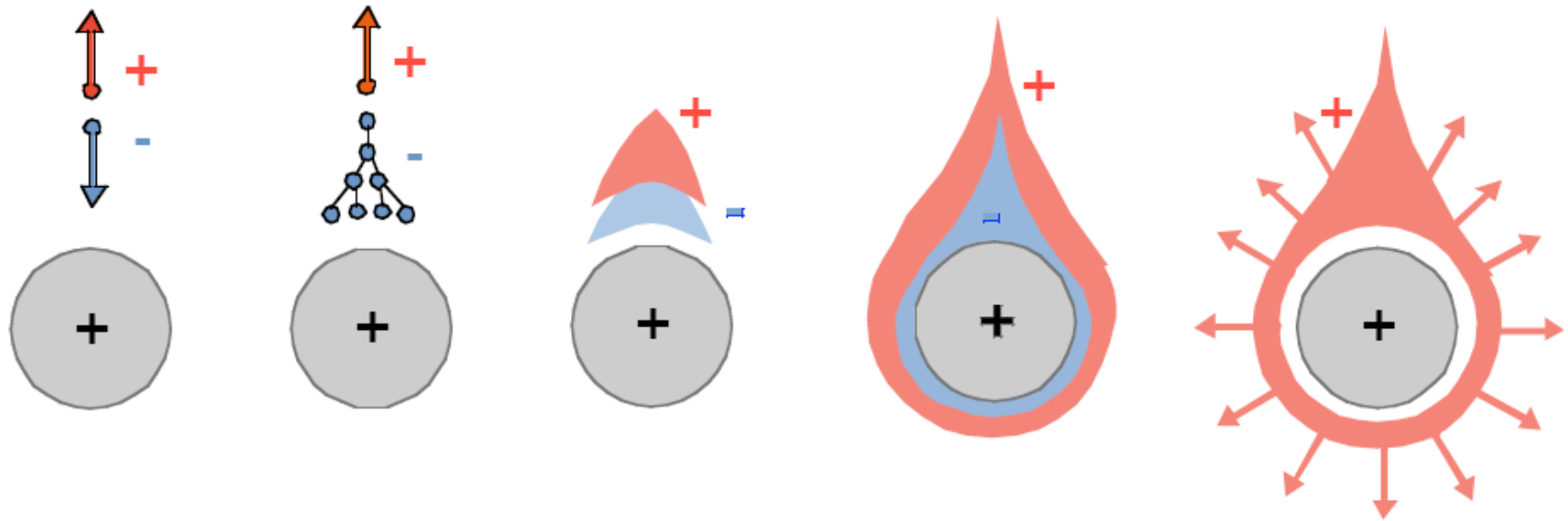


Combined cloud chamber-avalanche chamber:



H. Raether  
*Electron avalanches and breakdown in gases*  
 (Butterworth 1964)

## Signal development around the anode radius



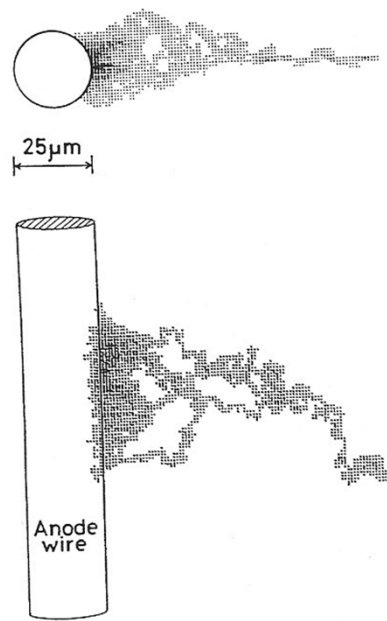


**Figure 6.5** Orthogonal views of an avalanche triggered by a single electron as simulated by a Monte Carlo calculation. The density of the shading indicates the concentration of electrons formed in the avalanche. (From Matoba et al.<sup>3</sup>)

Fig. 6.7. Basic configuration of a multiwire proportional chamber. Each wire acts as an independent proportional counter. The signal on the firing wire is negative while the signals on the neighboring wires are small and positive

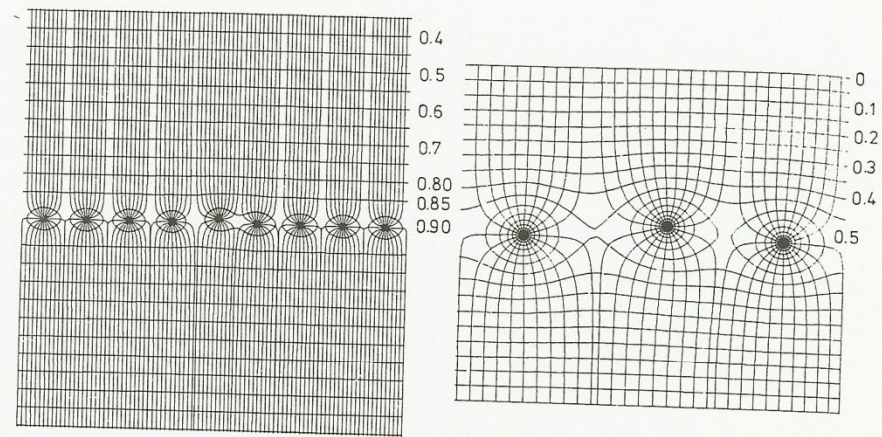
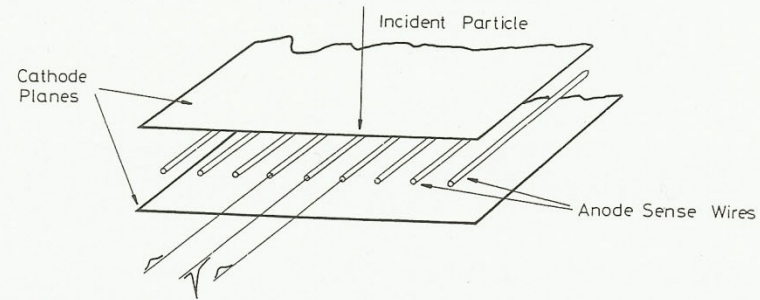


Fig. 6.8. Electric field lines and potentials in a multiwire proportional chamber. The effect of a slight displacement on the field lines is also shown (from *Charpak et al.* [6.16])

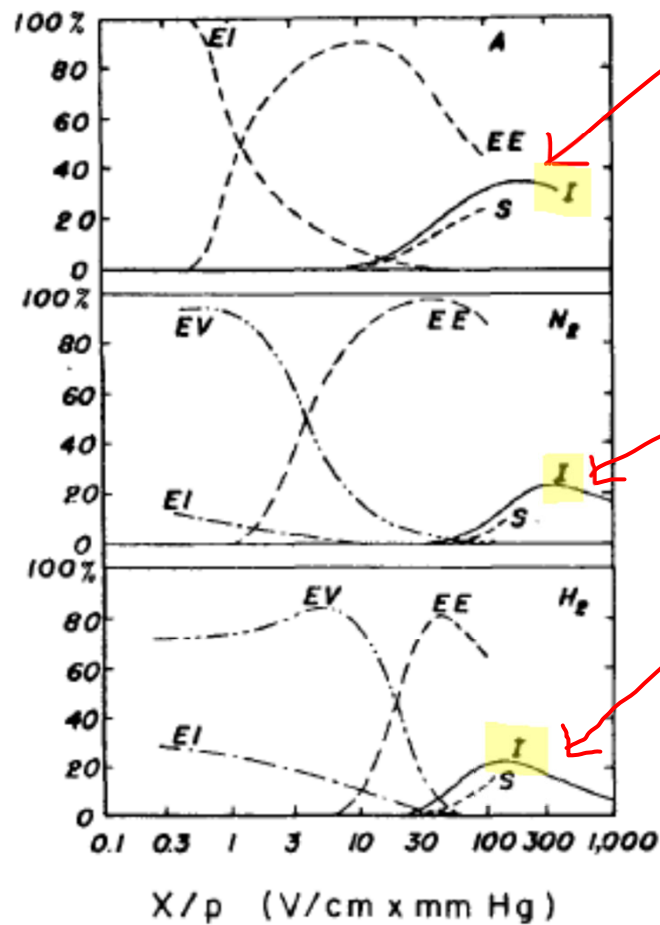


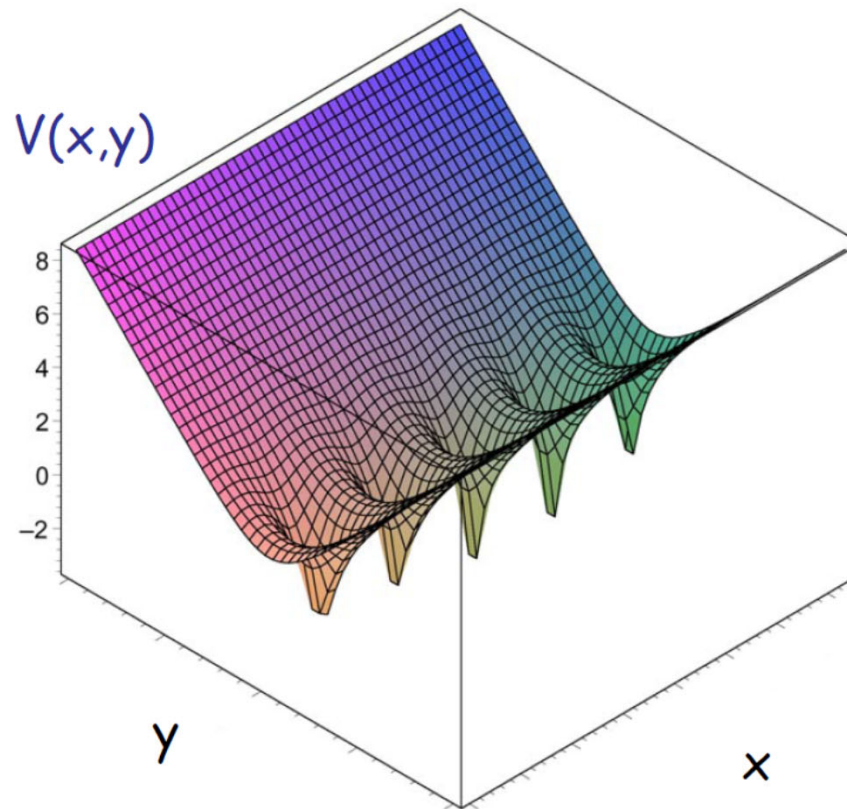
Fig. 43

Approximate curves showing the fraction of energy going into different processes in argon, nitrogen and hydrogen as a function of the reduced electric field<sup>16)</sup>. In the figure, EI represents the elastic impacts, EV the vibrational excitations, EE the excitations leading to photon emission and I the ionizations.

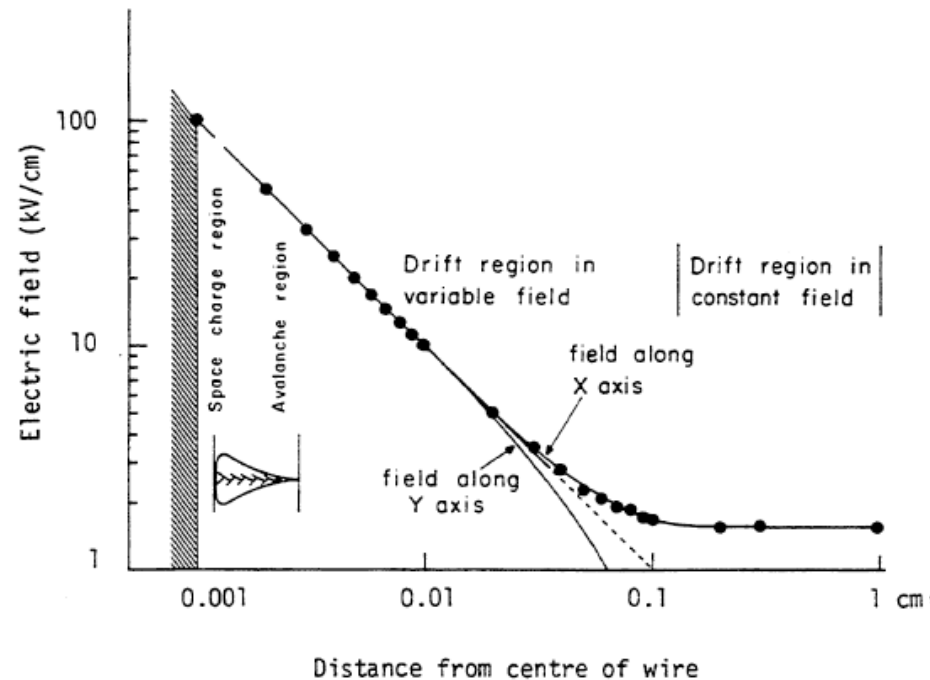
Strong field only around anode wires

Electrostatic potential in a planar MWPC given by:

$$V(x, y) = -\frac{q}{4\pi\epsilon_0} \ln \left\{ 4 \left[ \sin^2 \left( \frac{\pi x}{d} \right) + \sinh^2 \left( \frac{\pi y}{d} \right) \right] \right\}$$



## Strong field only around anode wires



- **scelta dei parametri**

- la camera è tanto più stabile quanto più il filo è sottile

- ragioni meccaniche limitano ad  $a=20\mu\text{m}$  a meno di camere molto piccole

- la spaziatura minima dei fili è 2mm

- valori inferiori tendono ad essere instabili elettricamente
- NB al diminuire di  $s$  diminuisce  $C$  e quindi il campo elettrico a parità di  $V_0$

- **Stabilità meccanica**

- variazioni percentuali di guadagno causate da problemi meccanici:

ricordando che

$$M \propto e^{cV_0} = e^Q \rightarrow \frac{\Delta M}{M} = \Delta Q \rightarrow \frac{\Delta M}{M} = \ln M \cdot \frac{\Delta Q}{Q}$$

dalla capacità per unità di lunghezza a  $V_0$  costante:

$$\frac{\Delta Q}{Q} = \frac{C'}{2\pi\epsilon_0} \frac{\Delta a}{a} \quad \frac{\Delta Q}{Q} = \frac{C'b}{2\pi\epsilon_0 s} \frac{\Delta b}{b}$$

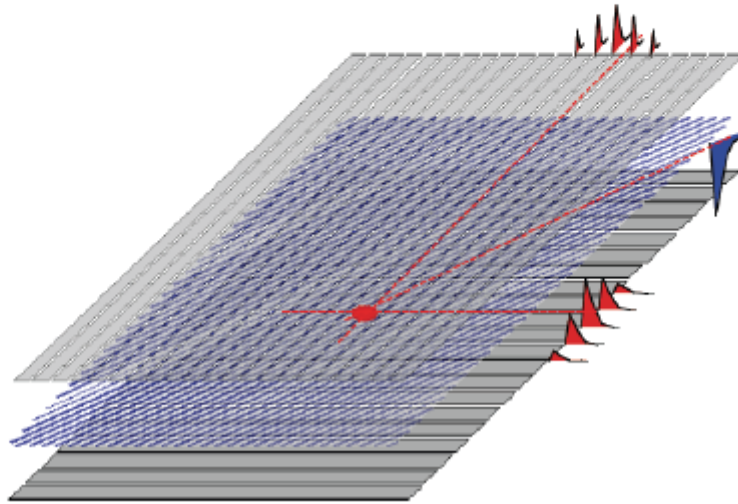
per valori tipici dei parametri:

$$\frac{\Delta M}{M} = 3 \frac{\Delta a}{a} \quad \frac{\Delta M}{M} = 12 \frac{\Delta b}{b} \quad \frac{\Delta M}{M} = 20 \frac{\Delta s}{s}$$

- è necessaria un'ottima precisione costruttiva e stabilità meccanica per avere guadagno uniforme
  - essenziale per misure di energia
- importanti soprattutto le forze elettrostatiche tra i fili



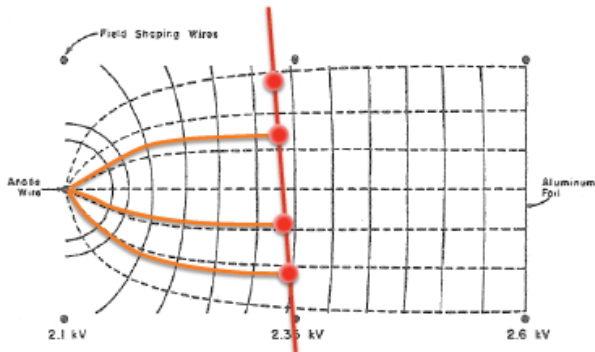
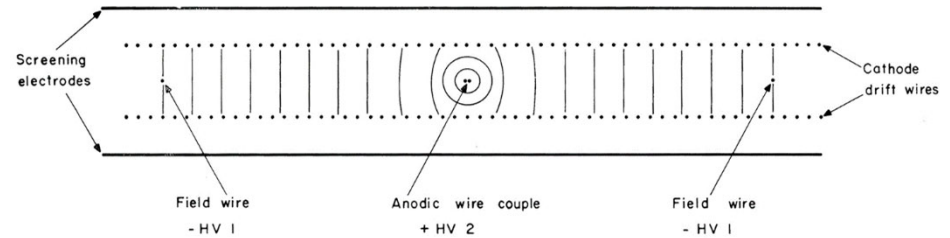
- Lettura catodica
  - catodo segmentato ortogonalmente ai fili
    - in genere larghezza delle strip  $\approx$  spaziatura anodo-catodo
  - si legge il segnale indotto sul catodo, che interessa più strips adiacenti



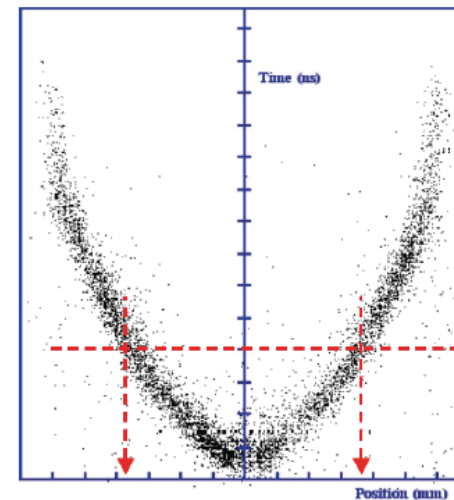
# Drift chambers

## risoluzione nelle camere a deriva

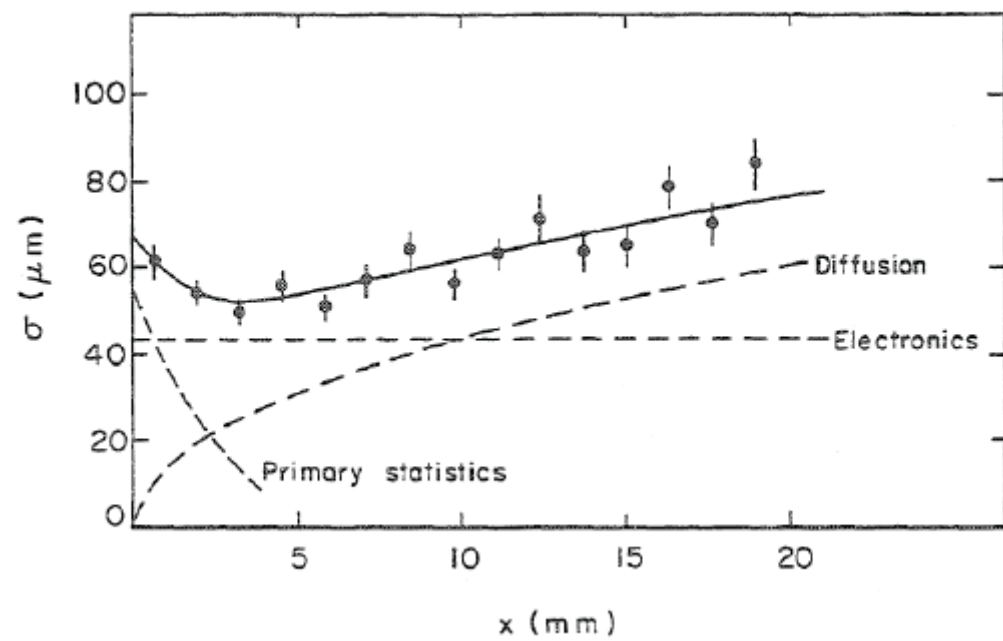
- tre effetti importanti
  - il rumore dell'elettronica
  - la diffusione longitudinale della carica
    - proporzionale a  $\sqrt{t}$  e quindi a  $\sqrt{x}$  per velocità di deriva costanti
  - la statistica di ionizzazione primaria



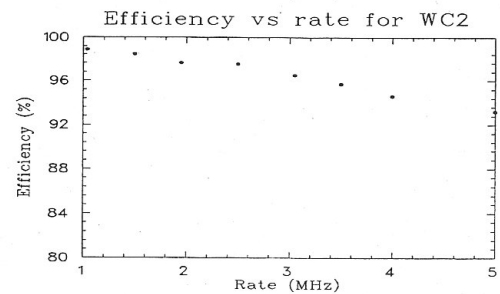
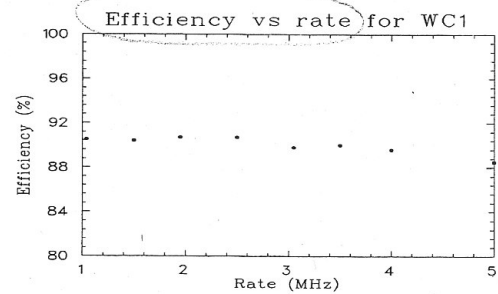
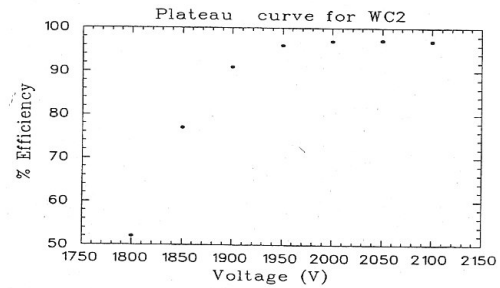
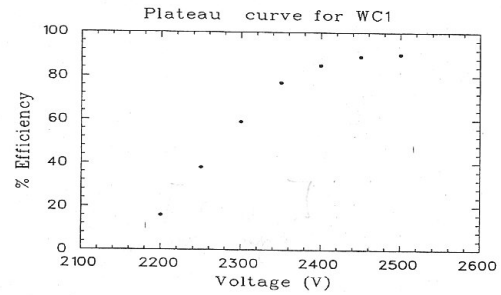
- i percorsi di deriva dei clusters di ioni sono diversi a seconda della posizione lungo la traccia
- effetto rilevante soprattutto per tracce vicine all'anodo



Left-right ambiguity



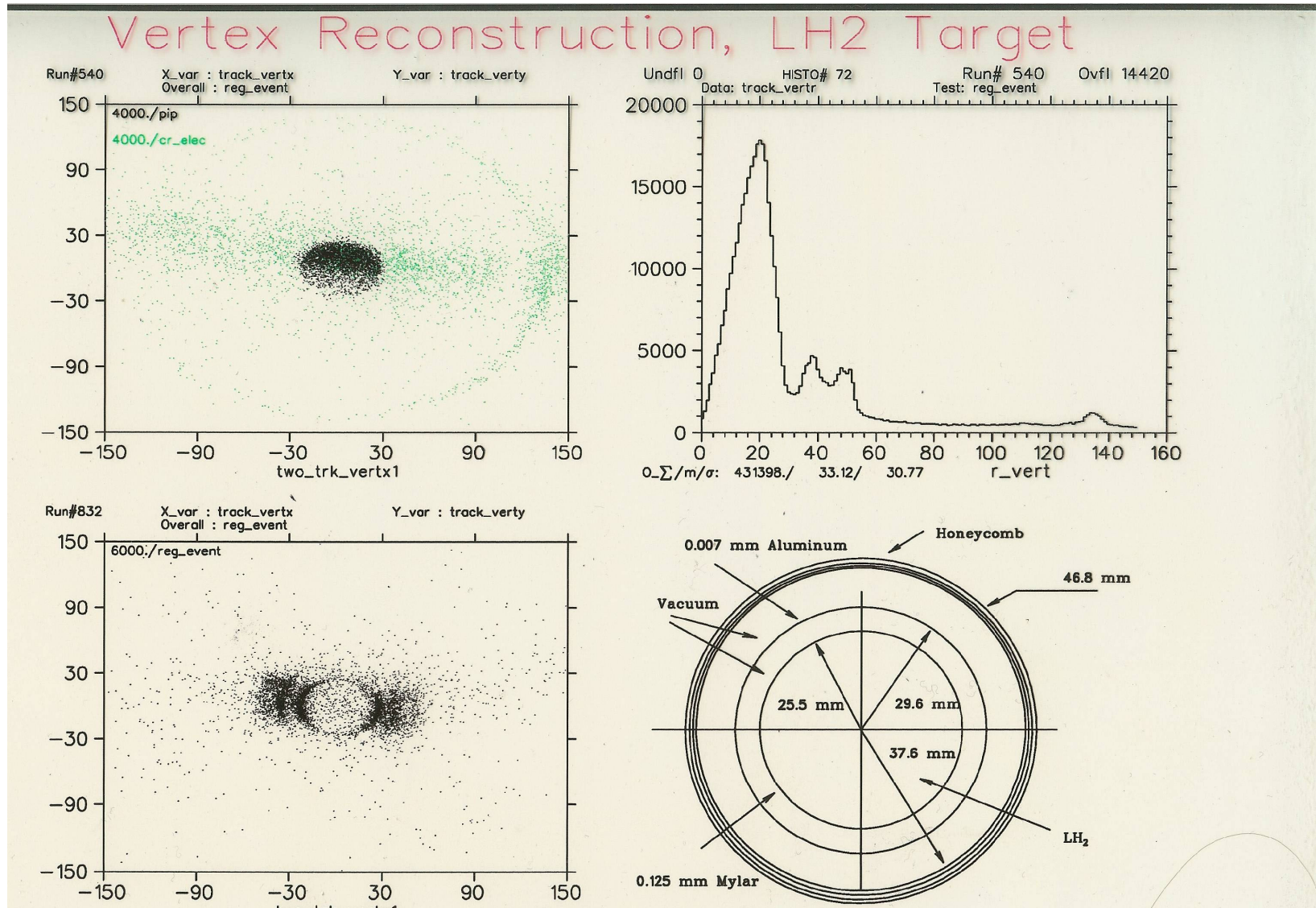
## Efficiency vs. voltage (gain)



## Efficiency vs. rate

Figure 3.6: The efficiency of WC1 and WC2 as a function of the incident beam rate is shown for operating voltages of 2450 V for WC1 and 2050 V for WC2, acquired with 225 MeV/c  $\pi^-$ .

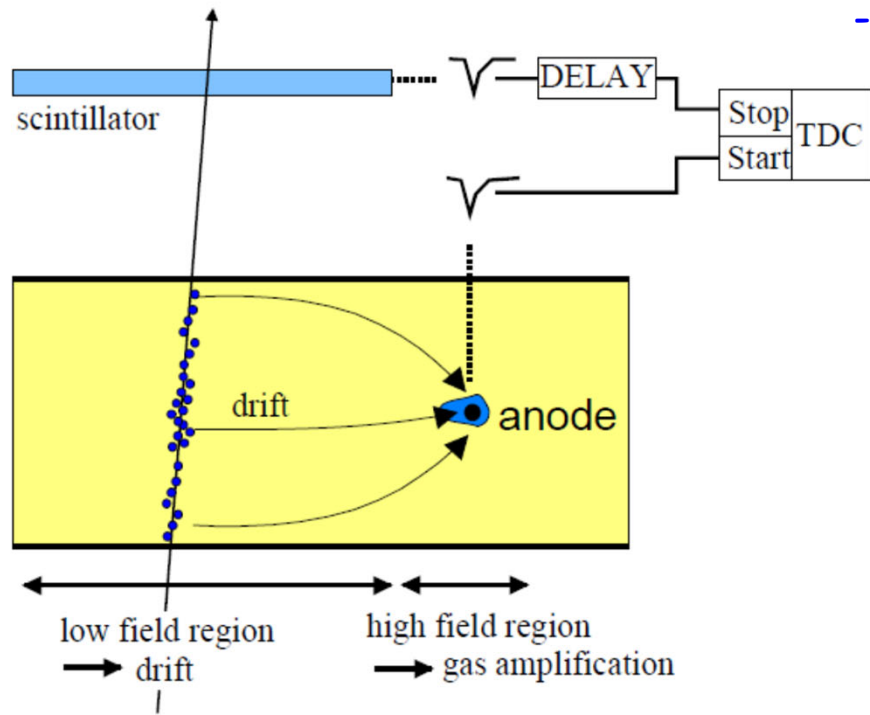
# MWPC applications: example of interaction vertex $\rightarrow$ tgt reconstruction



Start with Drift Chambers

Less wires than in a MWPC →

- Less electrostatic repulsion between wires (easier mechanics !)
- Less electronics



Resolution not limited by pitch

Measure the arrival time on wire

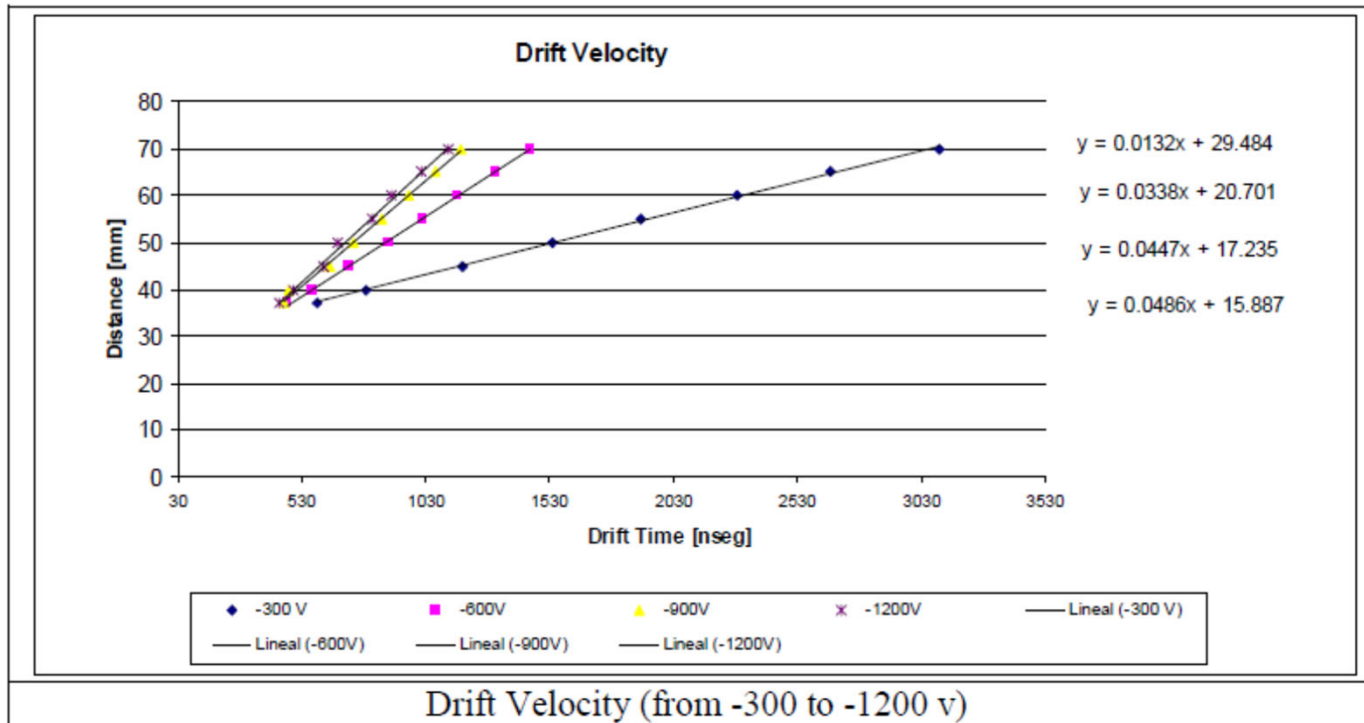
$$x = v_d(t - t_0)$$

Problems:

Resolution limited by thermal diffusion

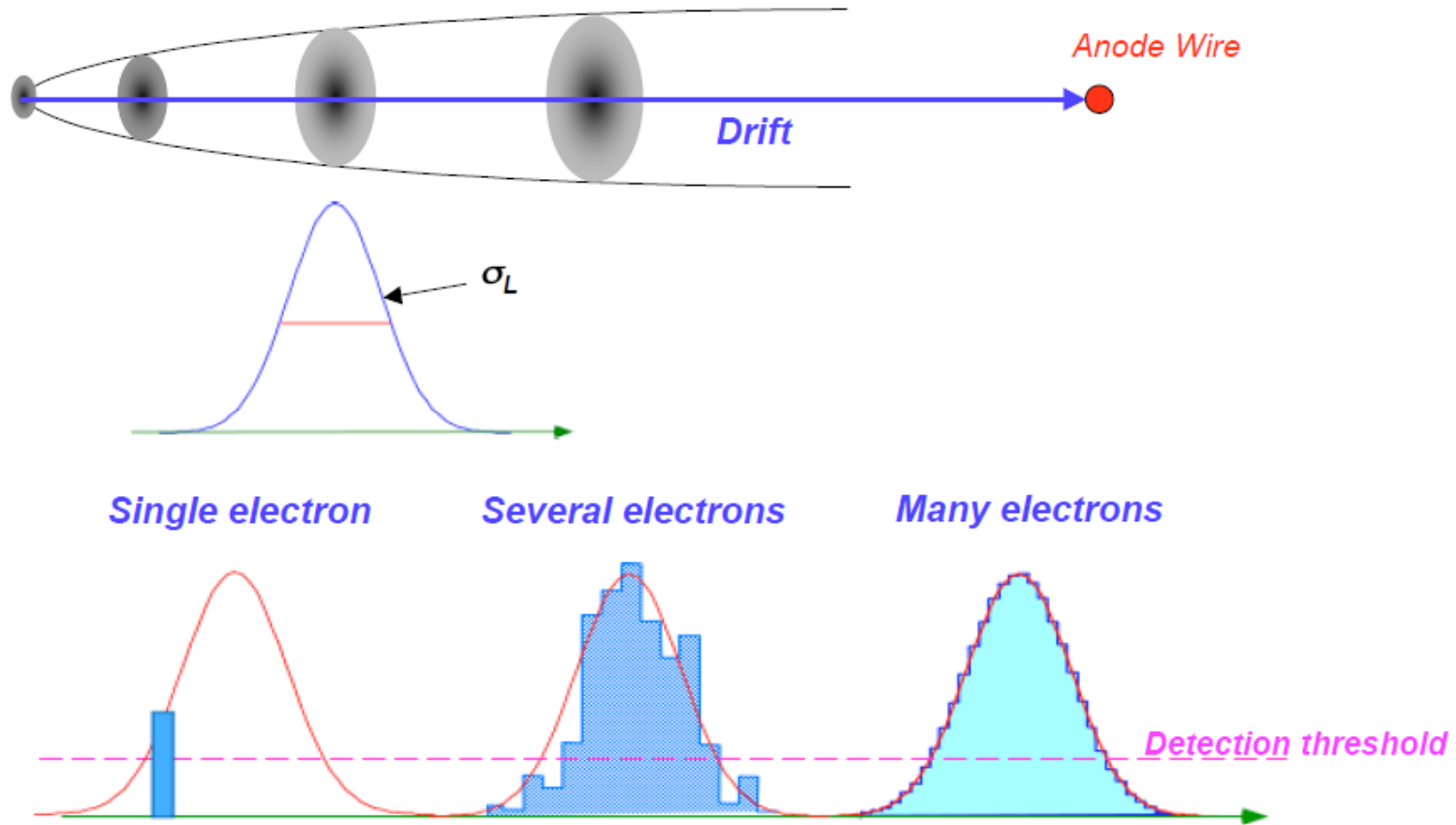
# Calibration of a Drift Chamber

## Position vs. time





**DRIFT TIME ACCURACY: DEPENDS ON IONIZATION DENSITY**



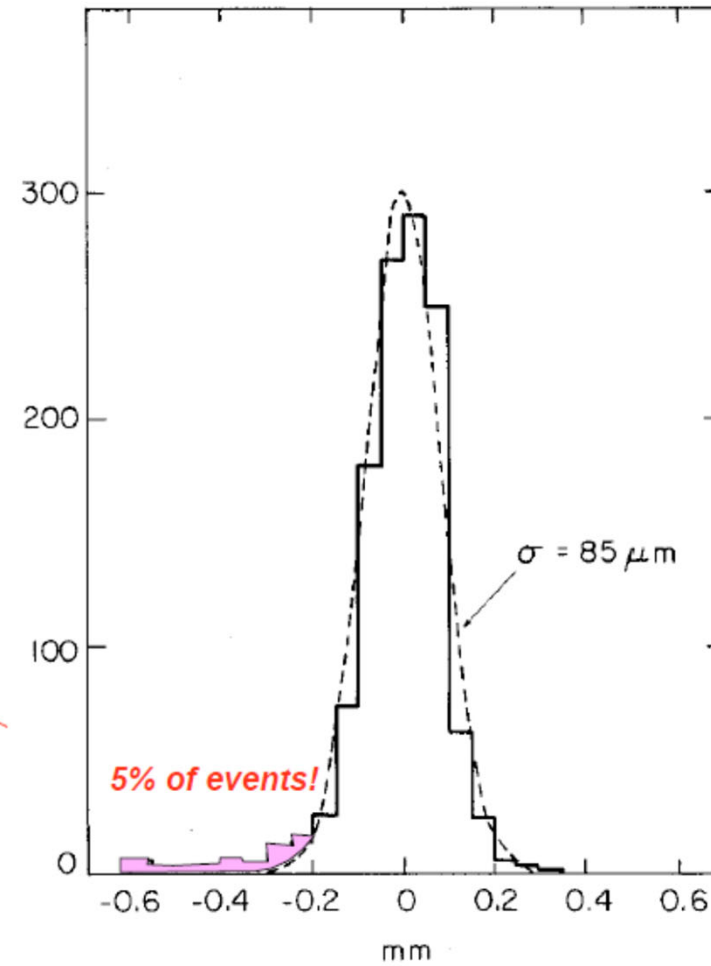
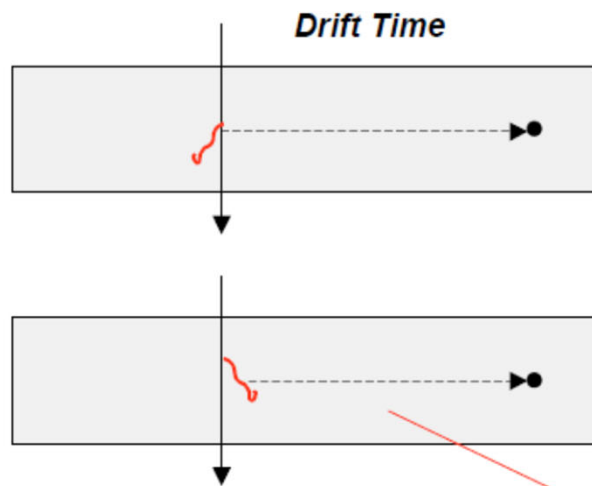
**Error on first electron electron:**  $\sigma_1 \sim \frac{\pi}{2\sqrt{3\ln N}} \sigma_L$      $N=100$      $\sigma_1 \sim 0.4 \sigma_L$

**RESOLUTION LIMITS OF DRIFT TUBES:**

G. Scherberger et al, Nucl. Instr. and Meth. A424(1999)495  
 W. Riedler et al, Nucl. Instr. and Meth. A443(2000)156



**LOCALIZATION ACCURACY IN DRIFT CHAMBERS  
WORSENERD BY LONG-RANGE ELECTRONS:**



# Time Projection Chambers (TPC)

Large volume active detector.

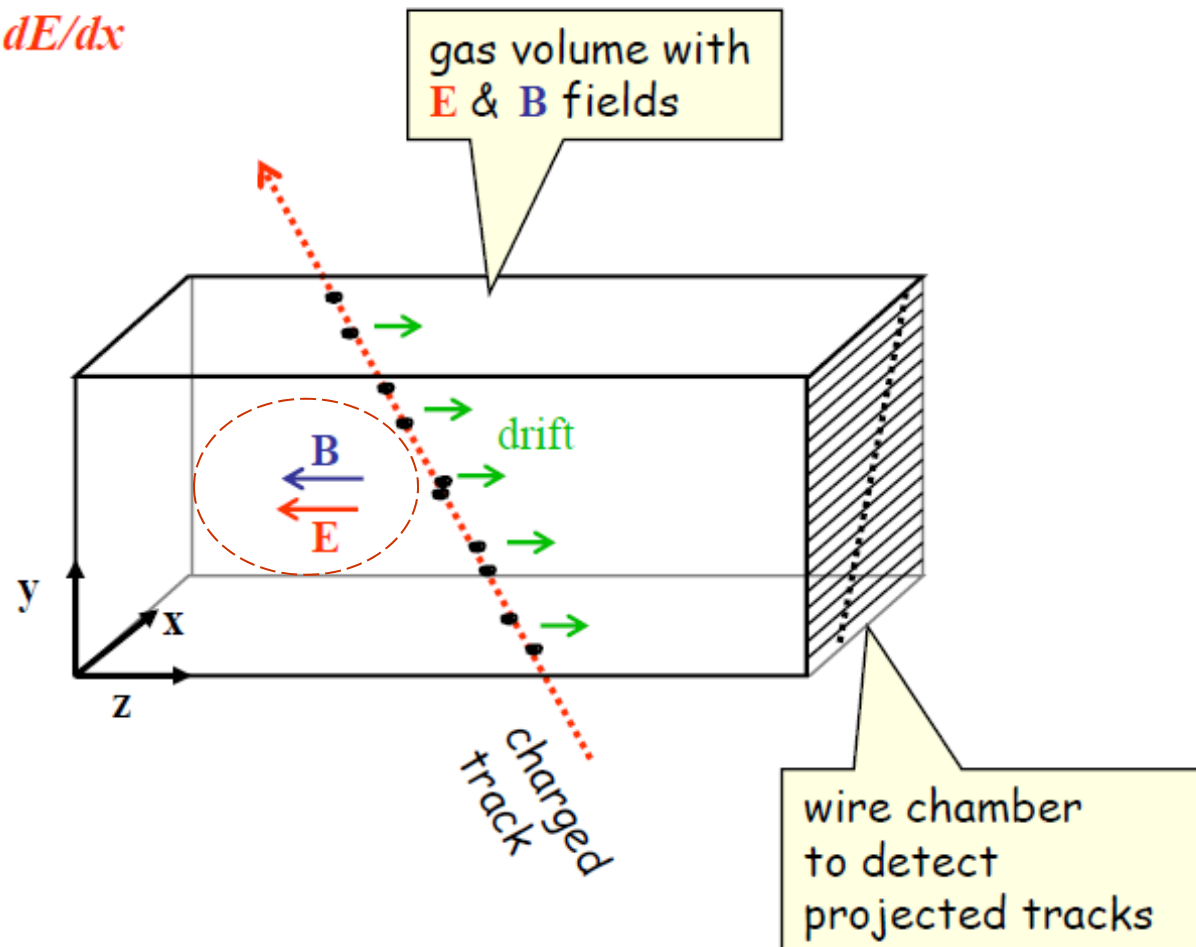
full 3-D track reconstruction

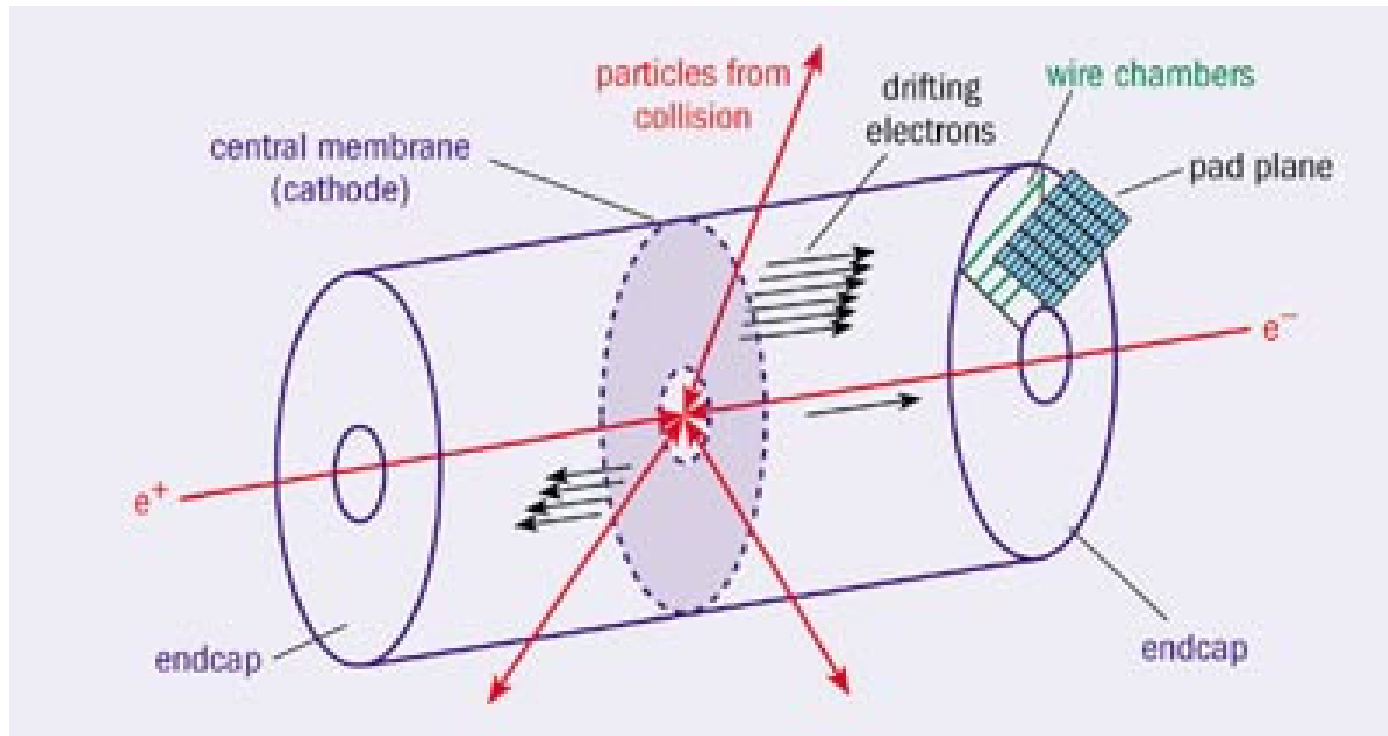
**x-y** from wires and segmented cathode of MWPC

**z** from drift time

and

$dE/dx$





6.8 The Time Projection Chamber (TPC)

143

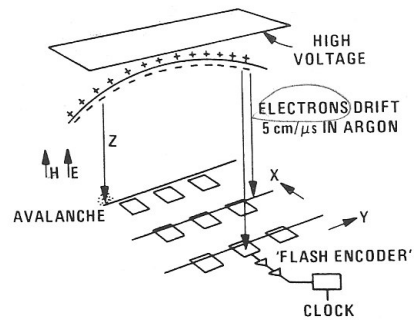


Fig. 6.18. Sampling the space points on a particle trajectory with the TPC (from *Lillberg* [6.31])

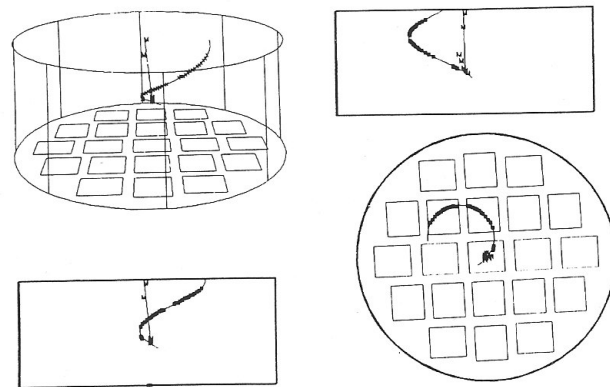
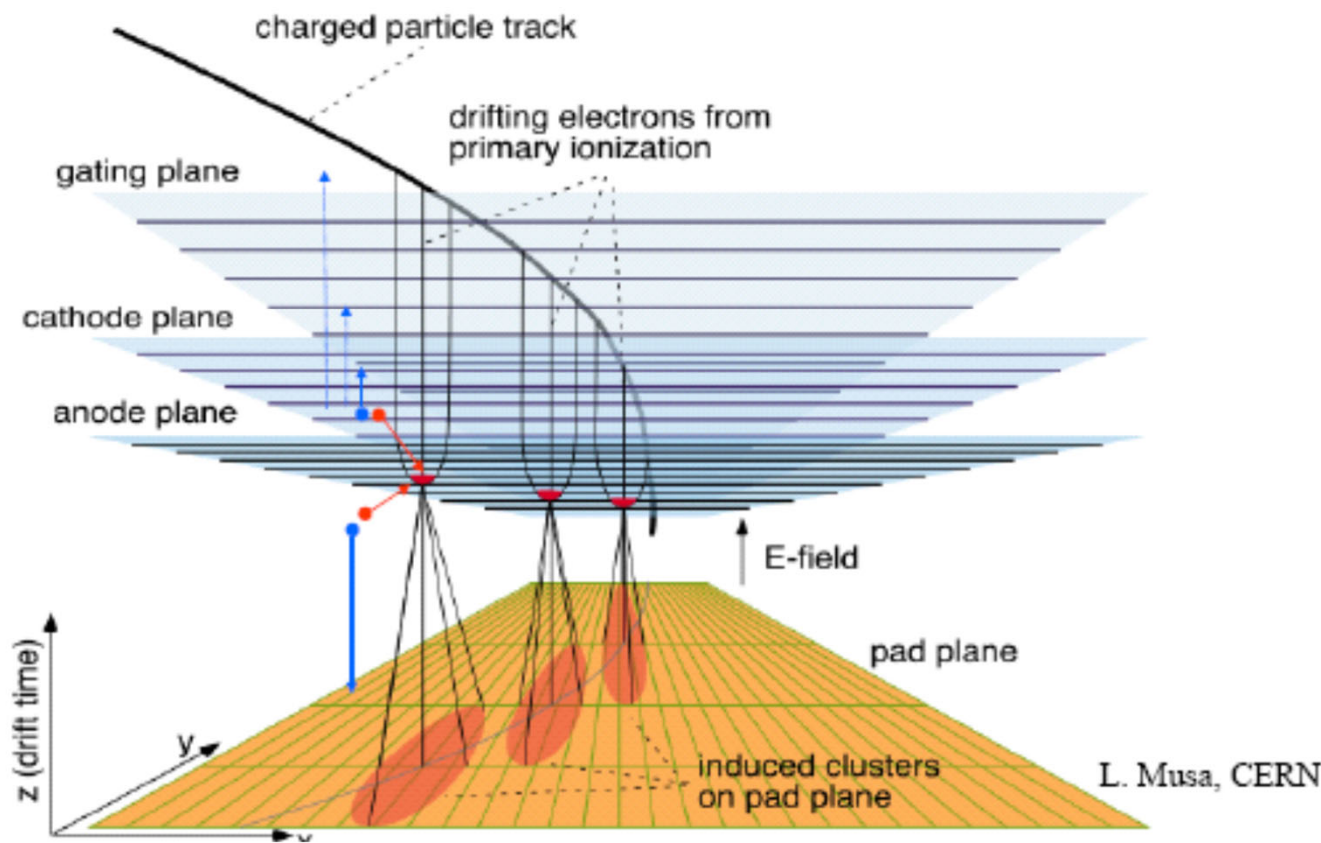


Fig. 6.19. Various views of TPC reconstructed tracks from an event in which an incident muon decays into a positron. The muon track is denoted by a *M* (from *Lillberg* [6.31])

## TPC WORKING PRINCIPLE



## More on TPCs

Usually  $B \parallel E$  improvement of diffusion

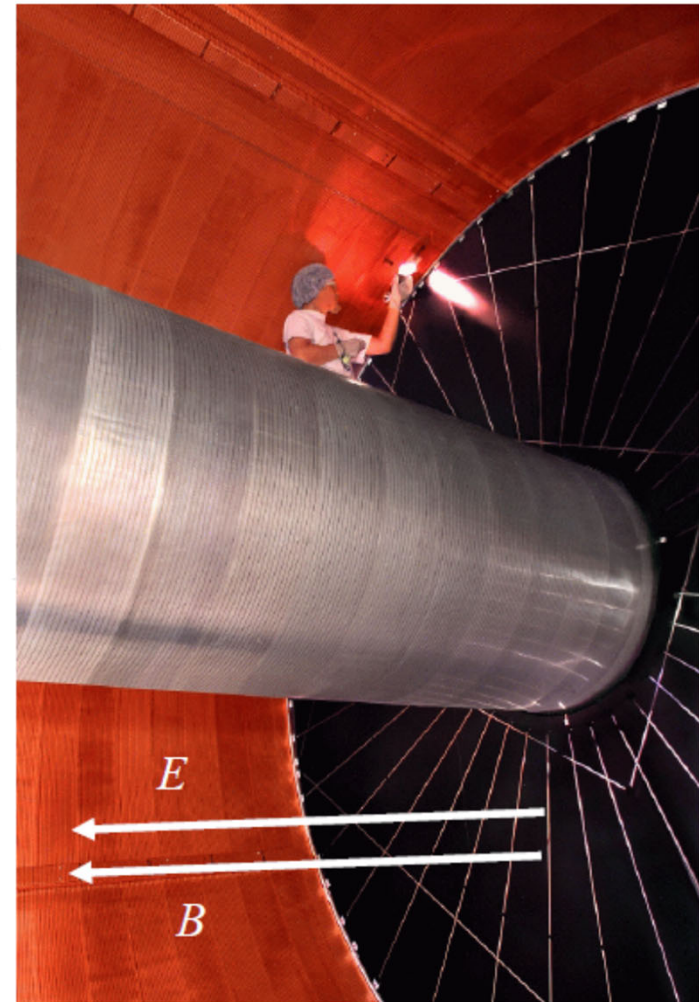
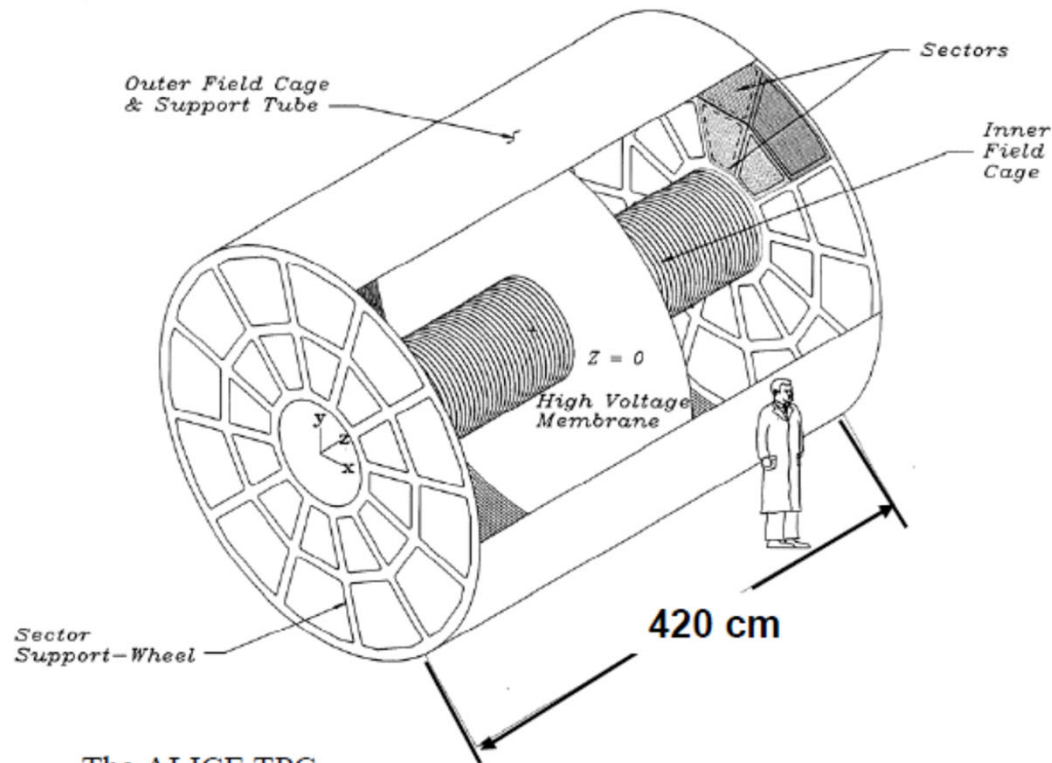
Drift length  $\geq 1\text{m}$

Rather (very) stringent requirement on homogeneity of  $E$  and  $B$  field

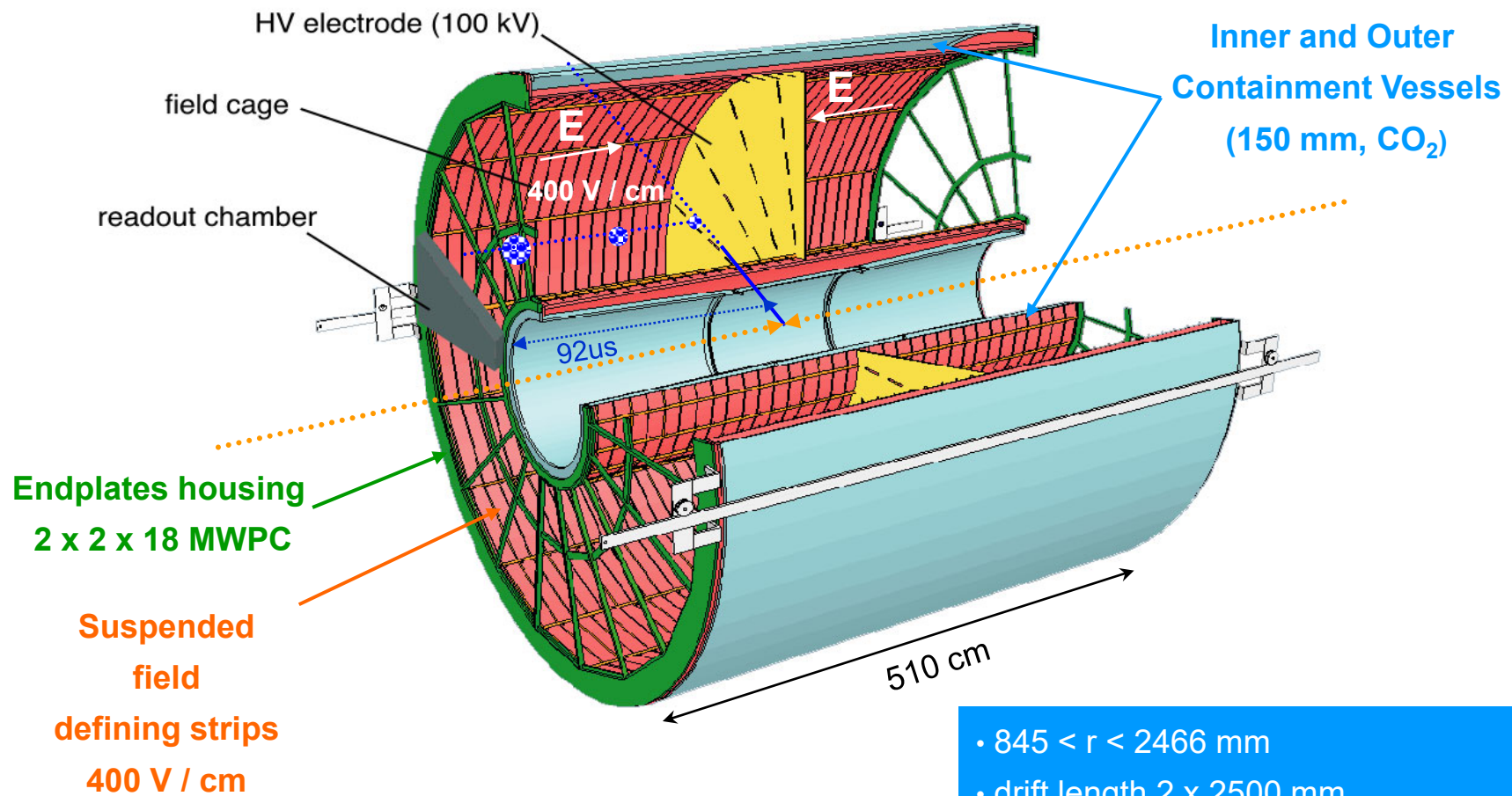
Space charge by ions

"Slow" detector

$$t_D \sim 10 \rightarrow 100 \mu\text{s}$$



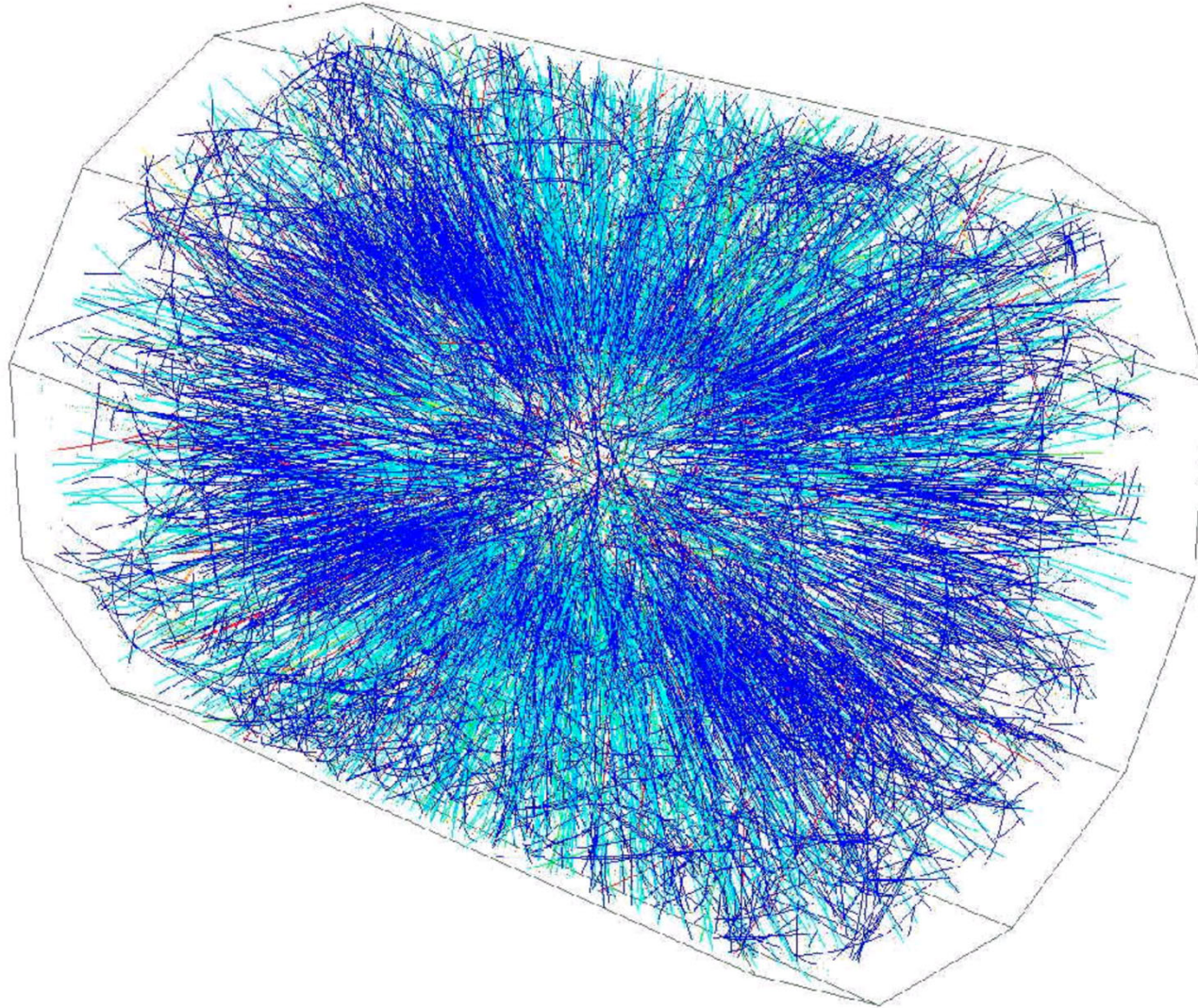




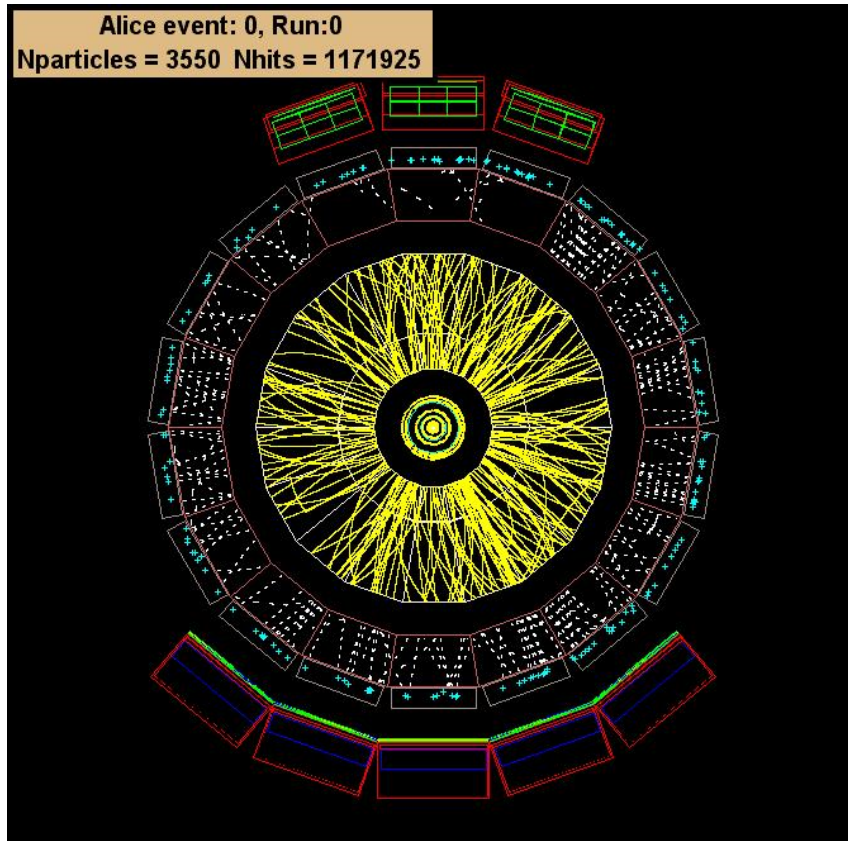
**ALICE TPC CHALLENGES**  
 up to  $2 \times 10^4$  charged particles in TPC

- $845 < r < 2466$  mm
- drift length 2 x 2500 mm
- drift gas Ne, CO<sub>2</sub>, N<sub>2</sub> (90/10/5)
- gas volume 95 m<sup>3</sup>
- 557568 readout pads

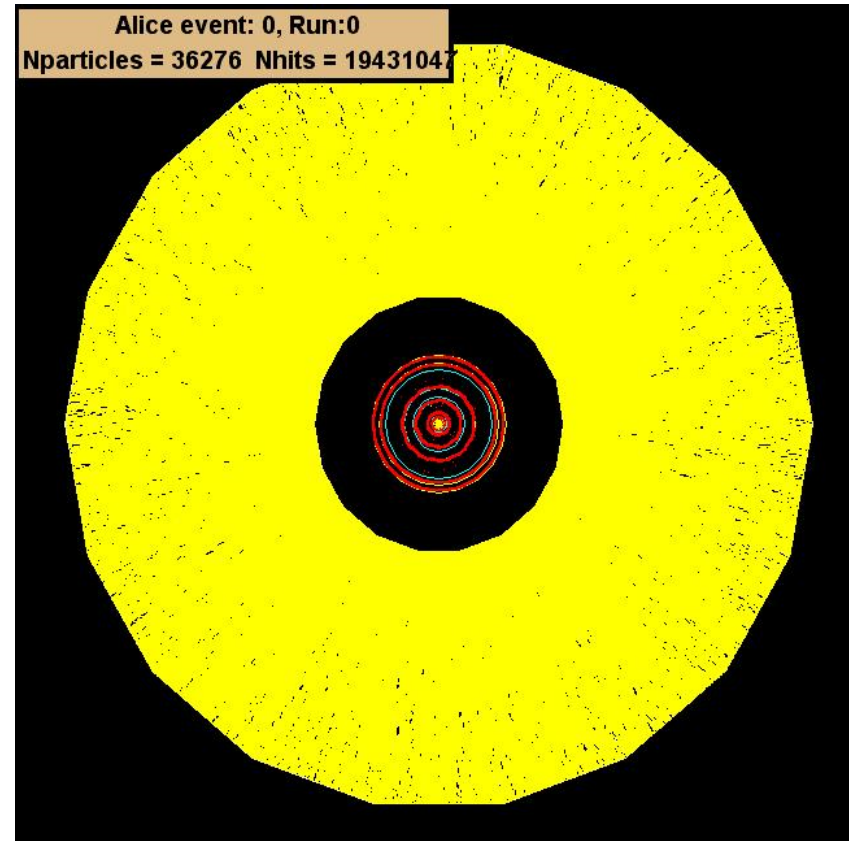
High multiplicity Au + Au  $\sqrt{s_{NN}} = 130$  GeV (STAR  
TPC)







$60^\circ < \eta < 62^\circ!$



One collision :  
 Pb+Pb @ 5.5 TeV  
 $dN/dy = 8,000$

